P1.32

THE EFFECT OF DIFFERENTIAL CLOUD COVER ON THE PROPAGATION OF A SURFACE COLD FRONT

James Correia Jr*
Raymond Arritt
Iowa State University, Department of Agronomy, Ames, IA

1. Introduction

Surface frontal behavior has been studied since the early 1950's. Sanders (1955) was the first to document an intense surface frontal zone. The development of fronts was largely attributed to synoptic scale dynamics. This viewpoint was extended as researchers were able to understand the radiation balance at the surface and distinguish between baroclinic zones and fronts.

Miller et al. (1996) gave a detailed mesoscale description of a maritime polar front that moved through the Midwestern US. Their primary findings included an enhancement of the thermal gradient due to daytime solar heating. This front was cloudy on the cold side and clear on the warm side. It displayed gravity-current like circulations of the type described by Segal et al. (1993, who performed idealized 1 and 2-D numerical simulations of fronts with and without clouds on the cold side of the thermal gradient. Their simulations suggested that thermal contrasts could be increased by 5K due to cloud cover during the daytime. The enhanced thermal contrast would induce gravity current circulations that enhance frontal lift at the leading edge of the front.

These studies have not diagnosed what happens at night when long wave radiational cooling might be affected by differential cloud cover. It is possible that differential cloud cover could create surface thermal contrasts due to differences in long wave radiational cooling. Here we model a cold front case which occurred on 12 August 2002, that moved through the upper Midwest. We also perform a sensitivity simulation in which cloud-radiation feedback is omitted to gain insight into cloud radiative effects on the front during both day and night.

2. Data and methodology

The Penn State University (PSU) Mesoscale Model version 5 (MM5) was used to model this event. The model was run at 40 km with an inner nest of 13.3 km centered over Iowa. Only the 40 km domain was analyzed here. The model configurations used are shown in Table 1. The newly employed NOAH LSM was used along with the simple cloud radiation scheme. A control (CTL) simulation and a no cloud radiation interaction (RAD) simulation were performed. Both simulations used the Betts-Miller convective parameterization, the Eta planetary boundary layer scheme and the Schultz microphysics package.

*Corresponding author address: James Correia Jr., Iowa State Univ., Dept. of Agronomy, Ames, IA 50010; e-mail: jimmyc@iastate.edu

3. Model simulations

3.1. Control Run

A strong 500 hPa moved towards Iowa as a predecessor disturbance initiated a squall line of severe thunderstorms. The Betts-Miller scheme realistically reproduced the synoptic situation. The precipitation amount during the simulation was relatively accurate compared to the 4km Stage IV multi-sensor precipitation dataset. The most significant issue facing this simulation was the "spin-up" for developing precipitation both temporally and spatially. Convection was occurring at the time of model initialization (12 Aug 2002 00UTC) over Kansas, Nebraska, and South Dakota. The model simulated this convection well but over predicted precipitation amount and coverage across Iowa in the first 12 hours. Although the rest of the simulation over predicted precipitation, it realistically predicted the spatial coverage at 6-hour intervals. A unique feature of the 24 hr precipitation forecast was a precipitation minimum associated with an MCV in Missouri (not shown). The initial over prediction of precipitation across Iowa can be attributed to a strong NW to SE oriented potential temperature gradient. This acted as a focus for upward motion and precipitation production.

The primary cold front was still in South Dakota by 12 Aug 06 UTC and moved slowly southeastward. As the front propagated, the magnitude of the potential temperature gradient decreased to background values but could still be followed. Isochrones of the leading edge of the front are shown in Figure 1. The front strengthened again at 13 Aug 06 UTC while propagating southeastward and was trackable until it stalled after 15 UTC.

A secondary gradient of potential temperature developed from 09 UTC to 12 UTC in this simulation and then decayed completely by 15 UTC (Figure 2). The gradient developed at and stays linked to the back cloud edge as the cloud layer prevents radiational cooling. This feature was found in the observations albeit weaker than the model. The squall line moved through Iowa by 18 UTC and the cold front began moving into Iowa. This cold front generated another area of convective rainfall at and behind the front. Cloud cover developed in the central portion of Iowa (on a SW to NE oriented axis) while the northwest portion became clear and calm (a situation favorable for long wave radiational cooling).

3.2. Simulation without cloud radiation interactions

The primary cold front exhibited similar behavior as in the control simulation. Notable differences include an inability to identify the front using the gradient of potential temperature from 18 UTC to 06 UTC. The front intensified by 09 UTC but it disagreed with the intensity and position of the front in the control simulation and observations.

The secondary gradient in potential temperature did not develop in the RAD simulation. This simulation produced similar cloud cover over the same area but there was no differential long wave radiational cooling. Direct comparison with the control simulation reveals a temperature excess of 2K in the control simulation under the cloud edge. This occurred because the simulation did not produce clouds in exactly the same area. Thus, the cloudiness in the control run inhibited long wave cooling of the area while such cooling occurred in the RAD simulation. This gradient developed in a matter of two hours and decayed just as quickly.

3.3. Hourly time series

Hourly time series of long wave radiation, lowest sigma level temperature, integrated cloud liquid water, and soil moisture at two points (one outside the gradient at 44N, one at the gradient 43.5N) for both model simulations were examined (Figure 3). The 2K difference between the points in the CTL run was 5 times larger than in the RAD run. Downward long wave radiation was about 60 W m^{-2} greater beneath the cloud-covered region of the CTL simulation. Outside the gradient however there was little difference between the CTL and RAD simulations.

The integrated cloud liquid water (ICLW) was used as a surrogate for cloud cover. Cloud edge was determined by ILCW of 0.009 m^3 kg^{-1}, a value that was subjectively determined by evaluating which contour best described the cloud edge without describing more random cloud fluctuations. Cloud cover explains the differences in temperature and long wave radiation between the CTL and RAD simulations. By 07 UTC, the RAD simulation decreased the ICLW (cloud cover) while the control increased ICLW. The enhanced cloud cover within the gradient for the next 2 hours allowed the temperature difference to increase. The loss of cloud cover by 13 UTC in both simulations allowed the temperature difference to erode as solar heating commences.

3.4. Cloud cover

The two simulations were compared for the distribution of cloud cover associated with the movement of the primary frontal zone. A subjective analysis revealed that the cloud cover in both simulations was nearly identical in shape and relative

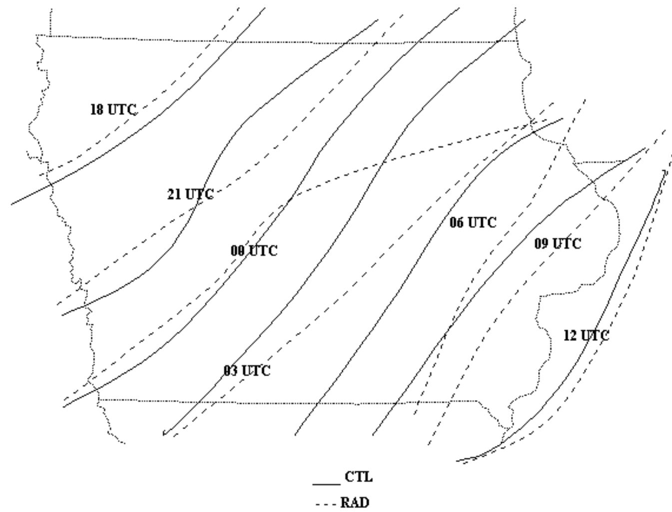

Figure 1: Frontal isochrone analysis from 12 Aug 2002 18 UTC to 13 Aug 2002 12 UTC. Solid line is CTL simulation and dashed line is RAD simulation.

position. Therefore, the RAD simulation did not have large effects on the cloud cover. Differences between the two simulations thus can be attributed to presence or absence of cloud effects on radiation rather than differences in cloud cover.

3.5. Frontal propagation

The primary cold front was tracked along its leading edge in the model according to both a temperature and wind vector analysis while pressure analysis was used as a secondary tool. The CTL and RAD simulation were relatively similar until 12 Aug 21 UTC. By 13 Aug 00 UTC a surface low formed along the front in the RAD experiment and skewed the frontal positions. Although a similar wave formed in the control simulation, it was 2 hPa weaker. The surface vortex extended aloft to 500 hPa in both simulations and was likely the result of convective feedback.

By 09 UTC the two fronts were once again in close proximity as the surface low moved northeastward. The isochrone analysis suggests that there is some diurnal component to the fronts movement. This can be seen from 6utc to 12 UTC in both simulations. The RAD simulated front slowed down drastically during the onset of solar heating, while the control run exhibited a more constant propagation. Although this is a subjective determination, the same type of movement occurred on 12 Aug 6 UTC to 18 UTC. The presence of convection during both periods demands further investigation.

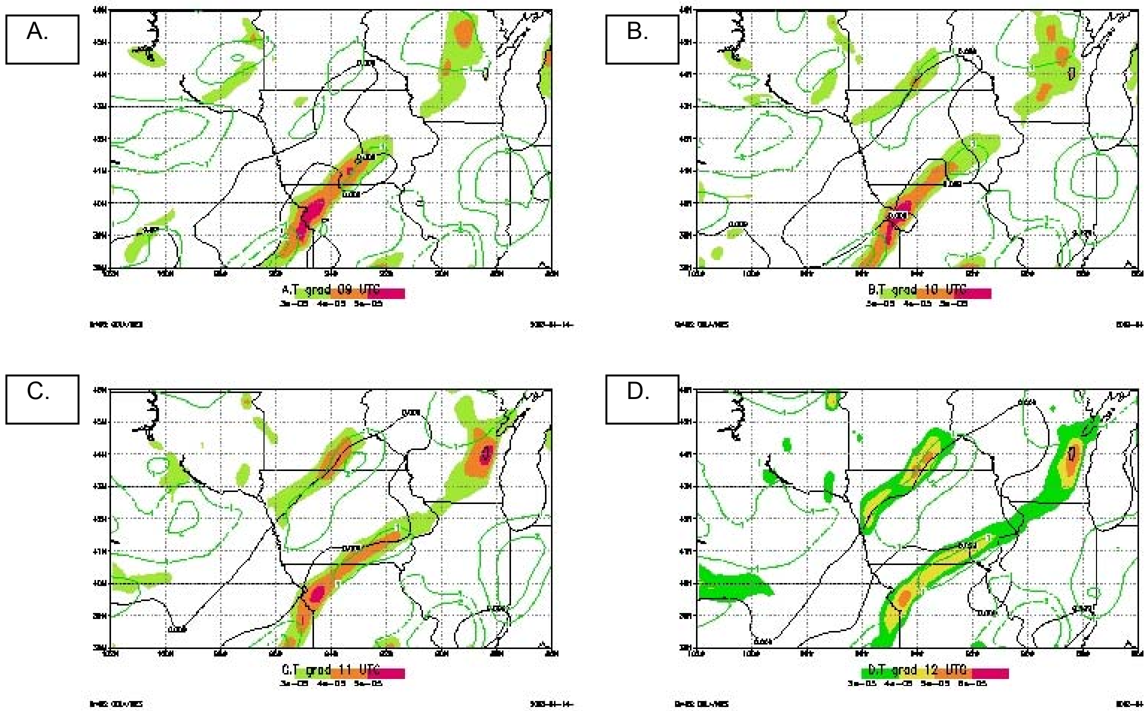

Figure 2: Gradient of potential temperature (shaded every 3 x 10^{-5} from 3 x 10^{-5}), temperature difference between CTL and RAD (light solid positive, light dashed negative at 1K intervals) and Integrated cloud liquid water (dark contour of 0.009 kg m^{-3}) at: A. 09 UTC B. 10 UTC C. 11 UTC D. 12 UTC

4. Conclusions

- The development of a secondary potential temperature gradient was dependent on long wave – cloud radiation interaction. The CTL – RAD comparison showed that a 2K difference developed across the trailing cloud edge. This is roughly one half the value reported by Segal et al. (1992) for day-time differential cloud cover thermal contrasts.
- Excessive precipitation occurred compared to observations. The model captured a precipitation minimum associated with an MCV.
- A surface vortex along the front was able to grow and cause a disparity in frontal propagation.
- The CTL simulation showed more frontal propagation from 00 to 06 UTC than the corresponding RAD simulation.
- Both model simulations reproduced the cloud field realistically around the front.

Acknowledgments

This research was funded by National Science Foundation grant ATM-9911417 and by Iowa Agriculture and Home Economics Experiment Station project 3803.

References

Miller, L. J., M. A. LeMone, W. Blumen, R. L. Grossman, N. Gamage, and R. J. Zamora, 1996: The low-level structure and evolution of a dry arctic front over the central United States. Part I: Mesoscale observations. *Mon. Wea. Rev.*, **124**, 1648-1675.

Sanders, F. and E. G. Hoffman, 2002: A climatology of surface baroclinic zones. *Weather and Forecasting*, **17**, 774-782.

Sanders, F., 1955: An investigation of the structure and dynamics of an intense surface frontal zone. *J. Meteor.*, **12**, 542-552.

Segal, M., W. L. Physick, J. E. Heim, and R. W. Arritt, 1993: The enhancement of cold-front temperature contrast by differential cloud cover. *Mon. Wea. Rev.,* **121**, 867-873.

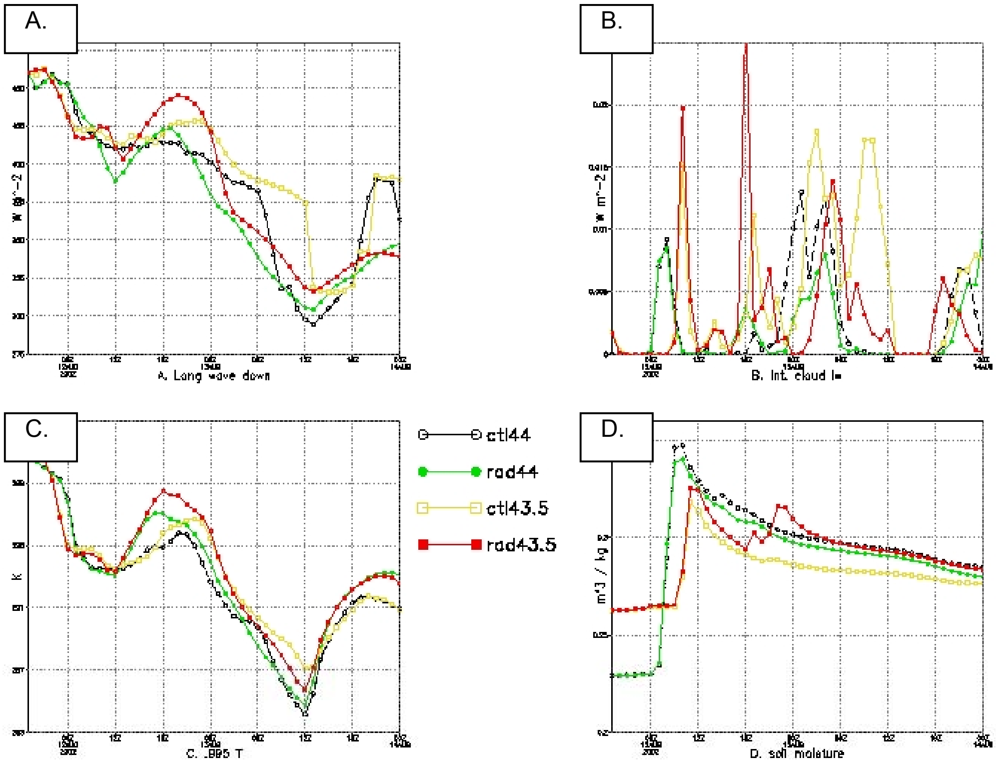

Figure 3: Hourly time series from 01 UTC 12 Aug. 2002 to 00 UTC 14 Aug. 2002 of A. Long wave radiation out (W m^{-2}), B. Integrated cloud liquid water (kg m^{-3}), C. Temperature on the lowest sigma surface (K), D. Soil moisture (m^3 kg^{-1}).